Chemical and Mineralogical Composition Analysis of Different Nigerian Metakaolins

Ike Chimdieze Daniel[a], William Ghann[b], Igboko Ndubuisi[a], Kenneth Okpala[a], Birol Ozturk[c], Mohammed M. Rahman[d] Faisal Islam Chowdhury[e], Md. Nuruzzaman Khan[f], Md. Rezaur Rahman[g], Md. Abdul Majed Patwary[h], Nafees Ahmed[i] and Jamal Uddin[b]*

[a]Chemical Engineering Department, Federal University of Technology, PMB 1526, Owerri, Nigeria

[b]Center for Nanotechnology, Department of Natural Sciences, Coppin State University, 2500 W. North Ave., Baltimore, MD 21216

[c]Department of Physics and Engineering Physics, Morgan State University, 1700 E. Cold Spring Ln, Baltimore, MD 21251

[d]Chemistry department, King Abdulaziz University, Jeddah 21589, Saudi Arabia

[e]Department of Chemistry, University of Chittagong, Chittagong, Bangladesh

[f]Department of Applied Chemistry and Chemical Engineering, University of Dhaka, Dhaka-1000, Bangladesh

[g]Department of Chemical Engineering and Energy Sustainability, Faculty of Engineering, University Malaysia Sarawak

[h]Department of Chemistry, Comilla University, Cumilla-3506, Bangladesh

[i]Department of Chemistry, Jagannath University, 9-10, Chittaranjan Avenue, Dhaka

Abstract

In this work, four different metakaolin samples (C01, A6060, B6075, and C12090) were investigated to determine their constituent elements and the relative quantities of the oxide contents associated with each of the elements. Kaolin samples were collected from different sites at Okpella, a village in the Edo state of Nigeria, West Africa. The metakaolin was produced by calcination at 750℃, which was followed by the dealumination process. The prepared samples were characterized by Field Emission Scanning Electron Microscope (FE-SEM), Energy Dispersive X-ray Spectroscopy (EDS), Fourier Transform Infrared Resonance (FTIR) spectroscopy, and X-ray diffraction (XRD) technique. Digital images were obtained and analyzed to determine the texture and porosity of the samples. FE-SEM images showed a slight difference in the morphology of the samples. Differing percentages of metal oxides were determined from the samples using EDS analysis. The major oxides present in all the samples were Silica (Silicon oxide) and Alumina (Aluminium dioxide). Aluminium was completely absent in C12090 but had a large percentage of silicon (36%).

Keywords: Clay, Kaolin, Oxides, Metakaolin, and Ceramics

* Corresponding author.
E-mail address: juddin@coppin.edu

1. Introduction

Kaolin is a hydrated Aluminum silicate clay having the empirical formula of $Al_2Si_2O_5(OH)_4$. Kaolin was first discovered in China in the 7th century and thus it is referred to as China clay. Kaolin particles are usually hexagonal in shape with an average size of 500 μm. [1]. The diameters of the particles usually range from 50 μm to 10,000 μm and generally contain silicon, aluminium, oxygen, iron, calcium, magnesium, sodium, potassium, phosphorus, and hydroxyl groups. Specifically, it is known to contain 48% of silicon dioxide (SiO_2), 38% of aluminium oxide (Al_2O_3), 1.72% of iron oxide (Fe_2O_3), 0.79% of calcium oxide (CaO), 0.72% of magnesium oxide (MgO), and 0.41% of titanium oxide (TiO_2). [2-6] These percentages may however vary depending on the types of the clay samples. [7] proposed a crystal structure with tetrahedrally coordinated silicon atoms and octahedrally coordinated aluminium atoms as displayed in Figure 1. [8] carried out density functional theory (DFT) calculations on the crystalline structure of Kaolin and reported that the inner hydroxyl groups were nearly parallel whereas the surface hydroxyl groups were slightly perpendicular.

Kaolin could be mined from different parts of the world including the USA, Brazil, and the UK. Kaolin samples are shown in Figure 2. They were obtained from Okpella, Nigeria. This type of clay consists of mainly Kaolinite and sometimes small amounts of other materials such as quartz, mica, rutile feldspar, and bauxite [9].
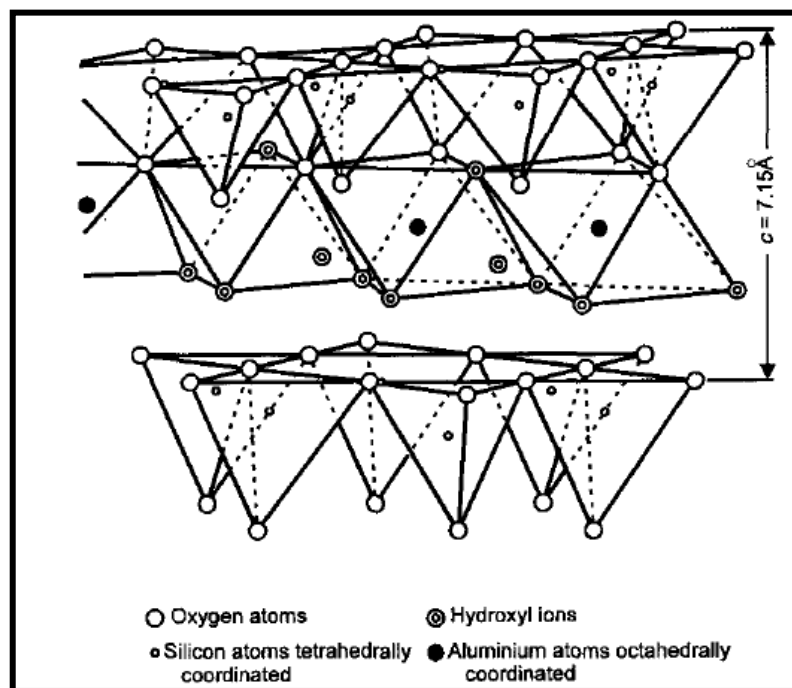

Figure 1. Kaolinite structure, adapted from Murray H. H. (1997) Applied clay mineralogy today and tomorrow, Clay Minerals (1999) 34, 39–49 [10]

Kaolin has a range of properties, making it valuable for several applications, including ceramics, cosmetics, toothpaste, food additives, paints, pharmaceuticals, desiccants, crayons, cement, enamels, DSSC sensors, and nanotechnology [11, 12]. However, the paper industry has the most use for Kaolin as fillers and coating on paper [13].

Kaolin is made of fine particles, is non-toxic, inert, and exists in different variations of the white colour [14]. Impurities in Kaolin causes off-white colouring hence, it is purified for certain applications [8,14, 15].

One of the many applications of kaolin clay is its use in the production of zeolites. Zeolites are important catalysts often used in the oil industry. Thus, the goal of this study was to purify and characterize Kaolin clay for developing zeolites. For all Kaolin samples, it is very important to determine the exact composition of the oxides present in the samples. Characterization of samples provides a means of categorizing them.

One critical step in the production of zeolites is the formation of metakaolin through the process of calcination. Production of zeolite occurs after calcination, dealumination, and characterization of resulting metakaolin. Metakaolins are very important and have several applications owing to their unique properties such as durability, resistance to chemical attack, diminished permeability and improved strength.

The specific goal of characterization studies carried out in this work was to determine the percentage of the various oxides present in the metakaolin samples. The samples were analyzed using Fourier Transform Infrared (FTIR) spectroscopy, Field Emission Scanning Electron Microscopy (FE-SEM), Energy Dispersive X-ray Spectroscopy (EDS), and X-ray diffraction (XRD) methods. FE-SEM imaging was carried out to study the morphologies of the samples.
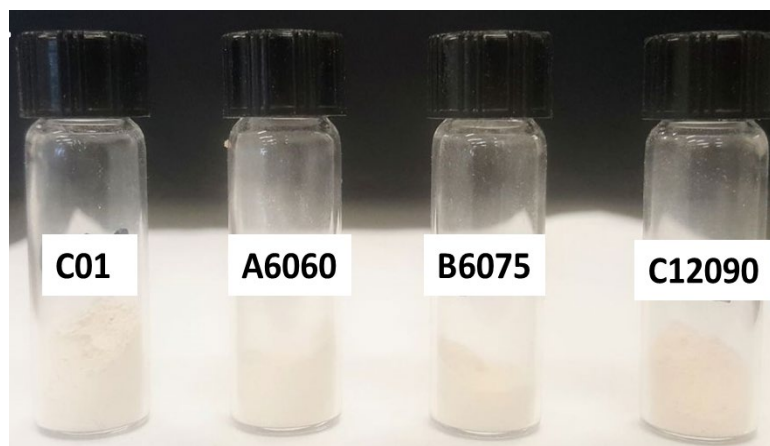

Figure 2. Metakaolin samples (C01, A6060, B6075, and C12090). analyzed in this study obtained from the Okpella mining site.

2. Experimental Procedure

2.1. Kaolin Clay

The Kaolin clay used in this research work was procured from Okpella village, Edo State Nigeria through the Freedom Group Mining Company. The Kaolin clay was termed as white and off-white raw Okpella Kaolin due to its mixed white and off-white appearance. The four different samples: C01, A6060, B6075, and C12090 were obtained from four different sites at Okpella village.

2.2. Size reduction of raw Okpella Kaolin

The raw materials were ground to reduce their sizes using a custom-made mortar. The reduced samples were sieved using a 75 µm sieve before calcination and analysis.

2.3. Calcination of Okpella Kaolin

The ground Kaolin was heated in a muffle furnace from drying state to calcination temperature of 750°C at the rate of 10°C/min and was held at this temperature for 15 minutes. Calcination was achieved by evenly placing the fine Kaolin into various crucibles to allow for good heat distribution since the specific heat capacity and latent heat of Kaolin was poor. The obtained metakaolin was placed in a desiccator for cooling prior to dealumination.

2.4. Dealumination of calcined metakaolin

The dealumination reaction required an external source of thermal energy to facilitate the dealumination of the metakaolin. About 16.3 grams of the metakaolin was mixed with 10M of H_2SO_4 in a conical flask followed by vigorous stirring to obtain a mixed slurry, which was then left to react in a water bath under manual stirring for 30 minutes at a temperature of 60°C. This procedure was repeated for all the samples at different reaction times of 60, 90, and 120 minutes and temperatures of 75°C and 90°C. At the end of each reaction, the samples were washed with a 10 M aqueous solution of $BaCl_2$. This step was performed to remove all the acid from the samples. Next, the samples were dried at 70°C in an oven. Each metakaolin sample was mixed with deionized water in a beaker to form a slurry, which was then poured into a measuring cylinder, serving as the settling tank. The size separation was achieved by allowing free settling of clay suspension in the measuring cylinder. A clay suspension was created from a mixture of clay and deionized water, whereas the settling time of heavier component (quartz) was determined from Stokes' Law equation based on the densities of particles and solvent (water), the viscosity of solvent (water), and the diameter of the particles (~20µm). The settled fine metakaolin clay was dried in the oven for 59 hours at 45°C and was packed into sample bottles for the next experimental stage.

2.5. Characterization techniques

The morphologies and compositions of all the samples were analyzed with X-ray diffraction (XRD) (Rigaku MiniFlex X-ray diffractometer, Rigaku Analytical Devices, Inc., Wilmington, MA, USA), a Field Emission Scanning Electron Microscopy (FE-SEM) equipped with Energy Dispersive X-Ray Spectroscopy (EDS) (JSM-7100FA JEOL USA, Inc). Attenuated Total Reflectance (ATR) spectra were obtained in the 4000 to 400 cm^{-1} range with a Thermo Nicolet iS50 FTIR. Digital imaging studies were carried out with a Celestron CMOS Camera from Celestron, Torrance, CA, USA.

3. Results and Discussion

3.1. X-ray diffraction analysis

Metakaolin samples compositions were characterized by using a Rigaku MiniFlex X-ray diffractometer (Cu Kα source, λ = 0.154185 nm). The X-ray diffraction (XRD) patterns of samples are shown in Figure 3. The high-intensity broad peak centred around 22° in all the XRD spectra, indicating the abundance of the amorphous SiO_2 phase in all samples. Major peaks of the C01 sample were observed at 2θ = 12.4°, 20.44°, 25.0°, 38.52°, and 62.36° corresponding to the (001), ($\bar{1}$10), (002), ($\bar{2}$02), and (060) reflections of the kaolinite minerals in the metakaolin samples, respectively [16, 17]. All the observed major peaks of C01 were in good agreement with the reported values for the kaolinite minerals in metakaolin (Al_2SiO_5) and the sharp peaks showed crystallinity. Additionally, XRD patterns of the samples A6060 and B6075 had both major peaks at 2θ = 25.0° and 68.4° corresponding to the (002) and (302) reflections of kaolinite minerals in metakaolin [18]. A6060

sample had another major peak at $2\theta = 40.25°$, corresponding to ($\overline{1}\overline{3}2$) reflection of kaolinite minerals in metakaolin. The other two major peaks of the B6075 sample were located at $2\theta = 48.2°$ and $60.25°$, which were associated with the (141) and (203) reflections of kaolinite minerals in metakaolin, respectively [17,18]. The sample C12090 displayed distinctive three major peaks at $2\theta = 20.8°$, $42.7°$ and $53.38°$ corresponding to (110), (041) and ($2\overline{2}2$) reflections of kaolinite minerals in metakaolin, along with smaller intensity diffraction peaks of the kaolinite minerals in metakaolin. [17,18]. The XRD analysis results indicated that all the metakaolin samples were mainly composed of crystallized kaolinite minerals and amorphous SiO_2.
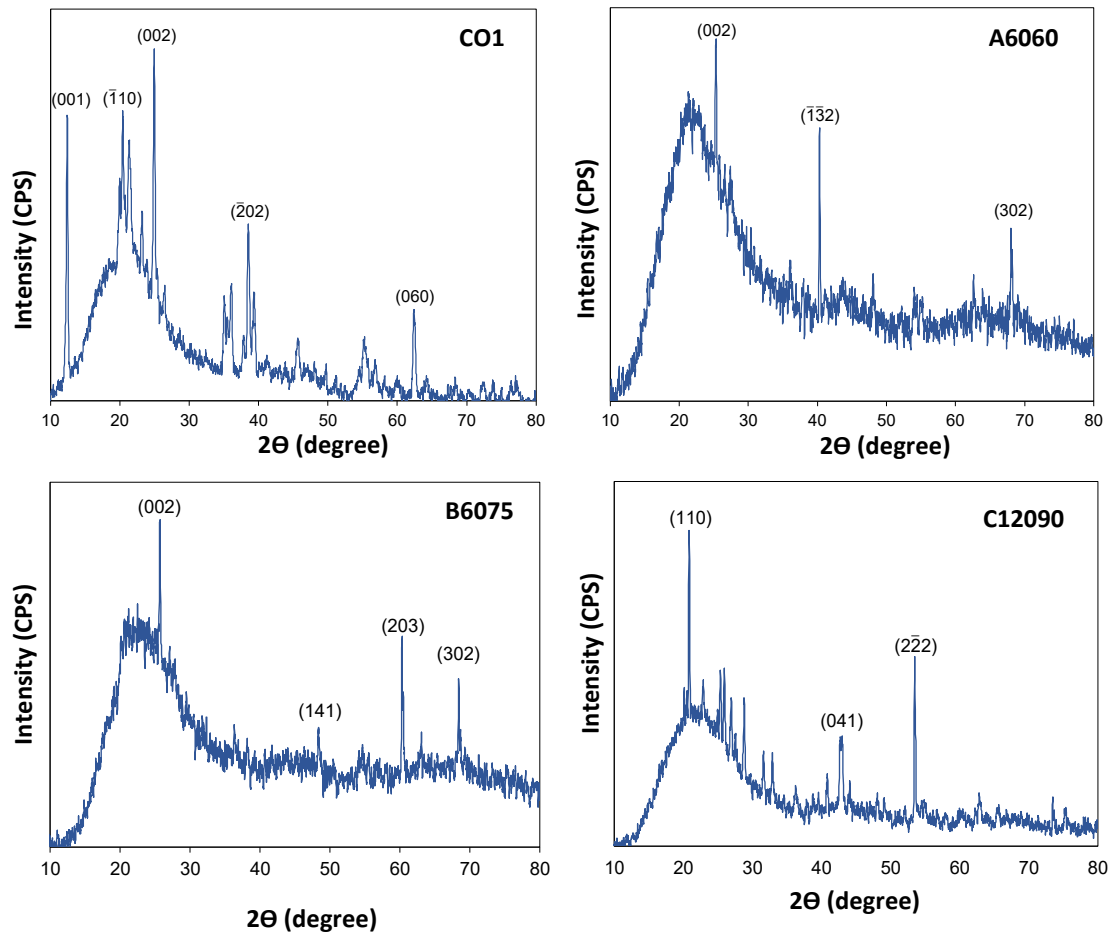

Figure 3. X-ray diffraction analysis of metakaolin samples.

3.2. Field Emission Scanning Electron Microscopy

The samples were also examined under the field emission scanning electron microscope (FE-SEM) to observe the differences in the microstructure at high magnification of the different metakaolin samples. FE-SEM imaging was an important tool for the understanding of the orientation and arrangement of the particles that were present in the metakaolin samples. [19,20] Figure 4 displays the FE-SEM images of the metakaolin C01, A6060, B6075, and C12090 samples at different magnification.
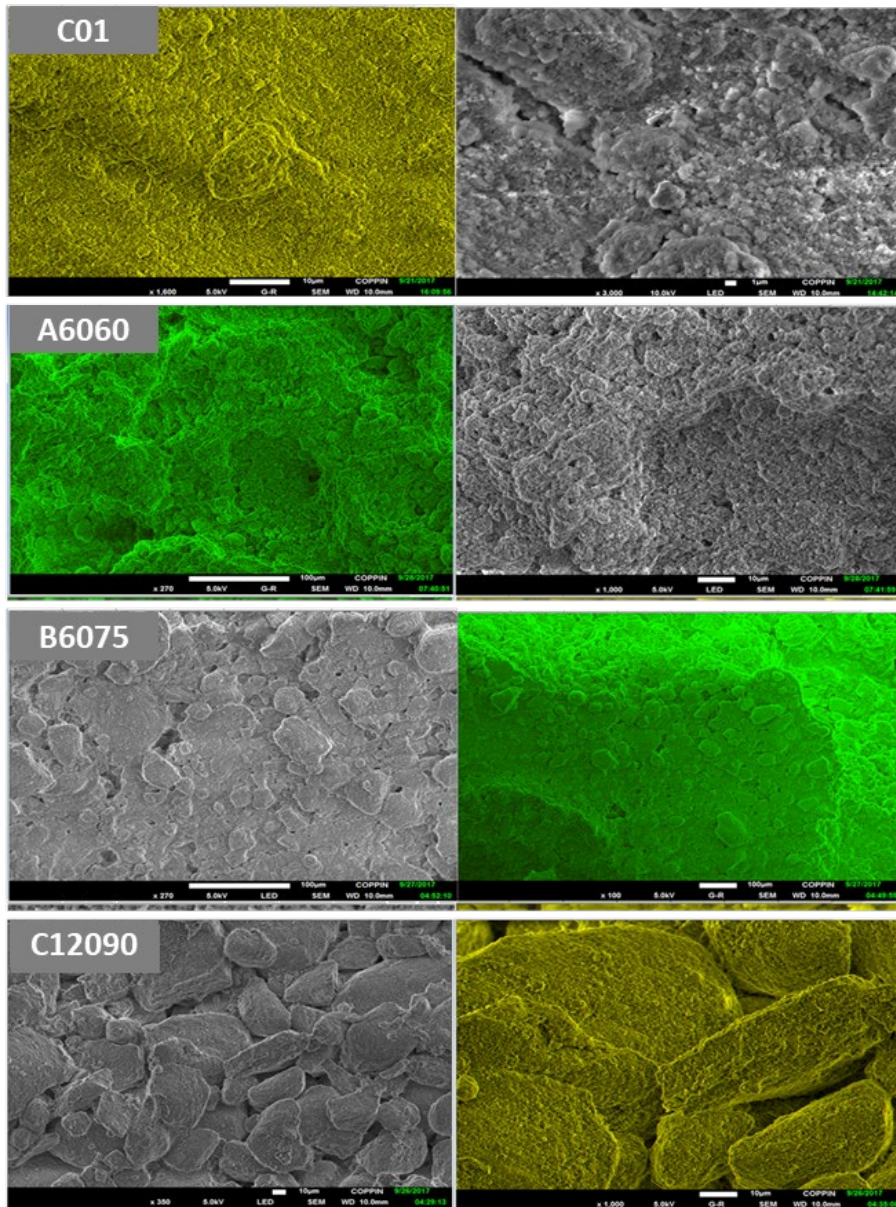
Figure 4. FE-SEM images of metakaolin C01, A6060, B6075, and C12090 samples taken at different magnifications showing their morphologies.

Metakaolin A12090 had distinct structures with clearly defined large grains in agreement with the digital imaging results. Metakaolin B6075 closely resembled A12090 except that the grains were more coagulated. Metakaolin C01 and A6060 showed similarities in their grain structures and appeared to have more spores compared to the other metakaolin samples.

3.3 Energy Dispersive X-ray Spectroscopy

The compositions of metakaolin samples were characterized with Energy Dispersive X-ray Spectroscopy (EDS) studies as shown in Figure 5. The four samples had varying amounts of aluminium oxide and silicon oxide. While there were equal amounts of alumina and silica in B6075,

C01 and A6060, alumina was almost absent in C12090, which agreed with the X-ray diffraction (XRD) results as explained above. The oxygen peak in relation to the metal was constant for all four samples. Aside from oxygen, silicon, and aluminium, there was no prominent peak representing other metals. In C01, it was observed that the peak for aluminium was slightly higher than that of silicon as was in the case of A6060. The silicon peak in spectra B6075 was however slightly higher than that of aluminium.

The ratio of the atomic concentrations of the elements of the four different samples was determined from the EDS spectra. The ratios for sample C01 were Si/Al=0.82, Si/O=0.23, and Al/O=0.28 and the ratios for sample A6060 were Si/Al=0.93, Si/O=0.35, and Al/O=0.37. The ratios of the atomic concentrations of the C12090 sample were markedly different since the Aluminum ratio was relatively low compared to other samples, as indicated by the low intensity of the Aluminum peak in the EDS analysis. The relevant ratio for Silicon and Oxygen was determined as Si/O=0.59. For all the samples, the main elements present by percentage mass were Oxygen, Silicon, and Aluminum.

These results were consistent with the typical elemental content of kaolin clays [21-23]. EDS and FTIR analysis indicated that the samples were mainly composed of silica and alumina with trace amounts of titanium, potassium, and sodium. Oxides of interest included SiO_2, Al_2O_3, Fe_2O_3, CaO, TiO_2, and K_2O as indicated by the peaks in EDS/FTIR scans.

3.4. Oxide contents of the metakaolin samples

The elemental analysis of metakaolin samples is given in Table 1. C01 metakaolin sample had mostly only oxides of Aluminum and Silicon with a very small percentage of Titanium. The average percentages by mass of this sample based on 10 measurements were 18.4 % for Aluminum, 15.1 % for Silicon, and 0.96% Titanium. These percentages were obtained through quantitative analysis via the Energy-dispersive X-ray spectroscopy.

Table 1. Percentage of Elemental composition of major elements present in metakaolin Samples.

Element	C01	A6060	B6075	C12090
Oxygen	65.99	56.59	57	61
Aluminum	18.43	21.22	19	-
Silicon	15.11	19.84	24	36

Thus, the ratio of aluminium to silicon in metakaolin C01 was 1.2:1. For sample A6060, the average percentages by mass, based on 10 measurements, were 21.2 % for Aluminum and 19.8% for Silicon, whereas the ratio of Aluminum to Silicon was derived as 1.1:1. B6075 metakaolin sample was mostly composed of oxides of Aluminum and Silicon with a small percentage of Sulphur (not displayed). The percentage by mass of the oxygen was 57% whereas aluminum and silicon were 19% and 24%, respectively. A12090 metakaolin sample was distinctly different from all the other metakaolin samples and had mostly silicon without any aluminium, showing that the sample was mainly composed of silicon oxide.
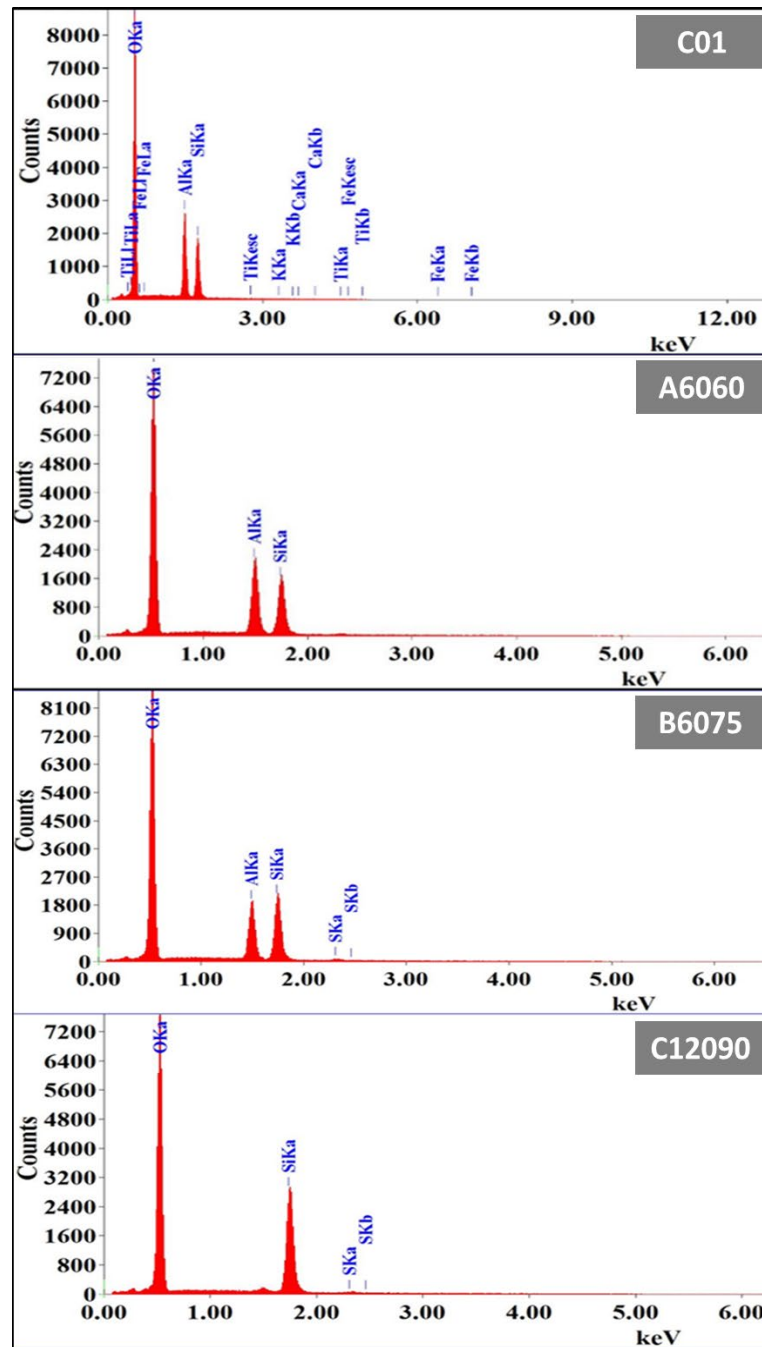
Figure 5. Energy Dispersive X-ray Spectroscopy (EDS) spectra of metakaolin C01, A6060, B6075, and C12090 samples.

3.5. ATR- FTIR spectroscopy

FTIR is one of the principal techniques used in the characterization of metakaolin and other types of clay. It is however not suitable for the quantitative determination of the components of metakaolin. Several absorbing bands associated with the FTIR of metakaolin have been reported in

the literature, where the main characteristic bands that had been generally reported included 3695, 3660, 3625, 1035, 1020, and 915 cm^{-1} [6, 24-27].

These peaks accounted for the -OH stretching, Si-O-Si, Si-O-Al and Al-OH bonds present in metakaolin. Figure 6 shows the FTIR spectra of the four different metakaolin samples investigated in this study. In these spectra, the bands between 3600 cm^{-1} and 3800 cm^{-1} denoted the -OH stretching band. The frequencies of -OH vibrations provided information on the identity of the cation linked with the hydroxyl groups in the sample. The absorbance band around 3600 cm^{-1}, displayed by metakaolin C01, and B6O75 samples, was indicative of a larger percentage of aluminium in the samples. The -OH stretching and crystalline hydroxyl were also present in the same region. A broad absorption band around 1038 cm^{-1} was indicative of the presence of silicon dioxide, accounting for Si-O stretching in clay materials [27-34].
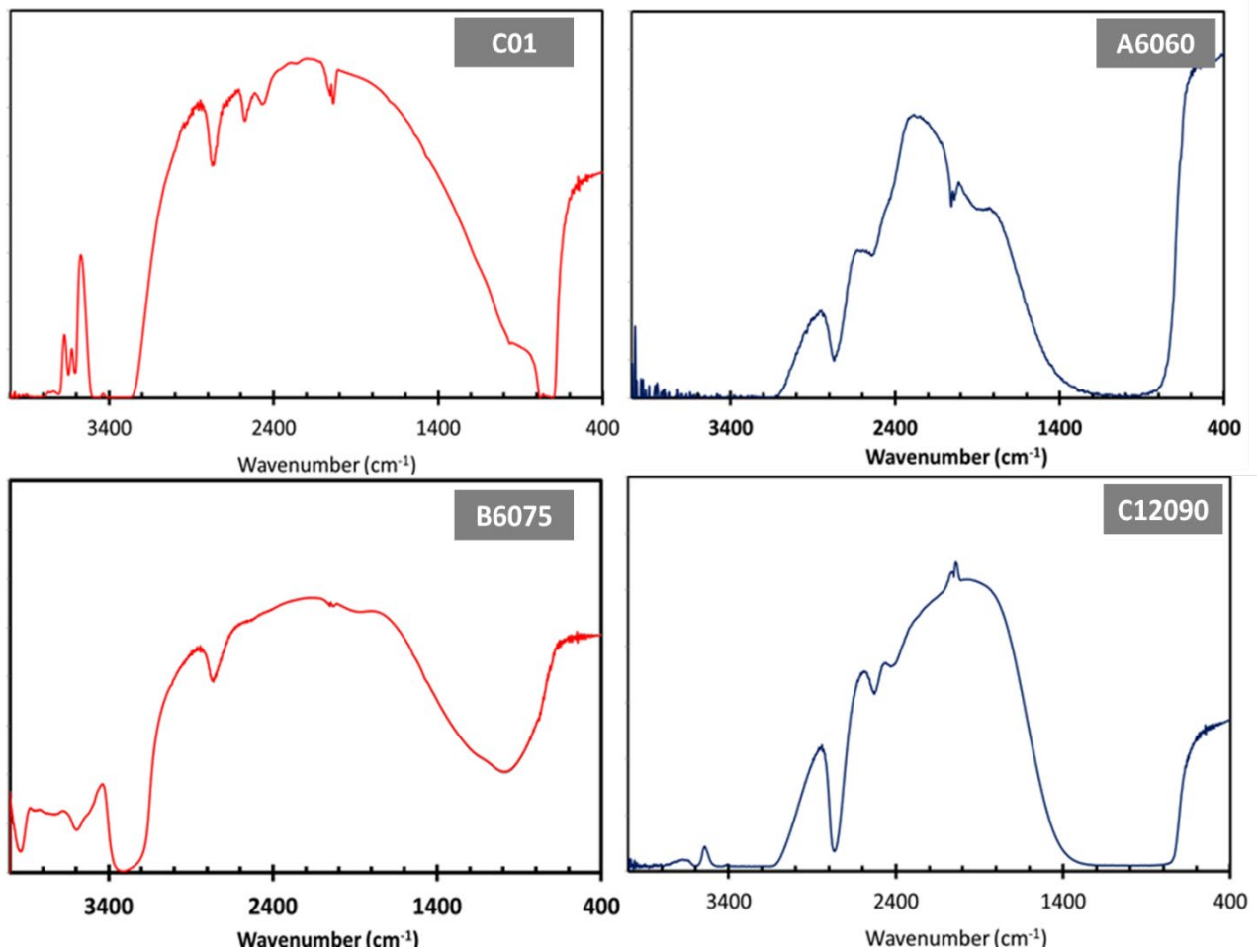

Figure 6. Fourier transform infrared (ATR-FTIR) spectra of four (C01, A6060, B6075, and C12090) different metakaolin samples.

3.6. Digital Imaging Studies

Digital images of the samples were captured to compare the physical appearance, morphology and porosity of the samples. As shown in the digital images in Figure 7, all the samples displayed off-white colour and similar morphology. Metakaolin is white in colour when it is pure. Therefore, the off-white colour was indicative of the presence of impurities in the samples. The particles were seen as

irregularly shaped and of different sizes. The C01 sample was very grainy compared to the other samples and C12090 showed their morphology. Some coagulation at various points was observed in the metakaolin samples. B6075 and A6060 seemed to have the same kind of texture. The grains of A12090 were coarser compared to other samples.
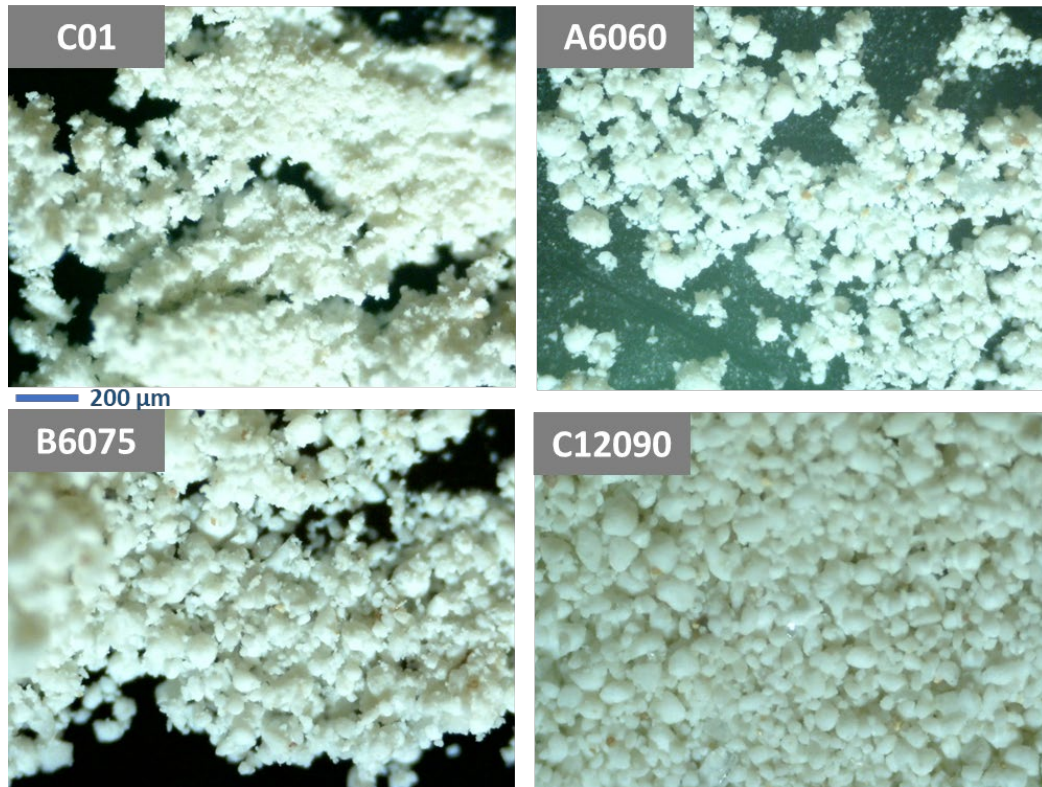

Figure 7. Digital images of the metakaolin samples (C01, A6060, B6075, and C12090).

4. Conclusions

The present study dealt with the preparation and characterization of metakaolin for application in various fields of study. Metakaolin is a very important clay that is used in a myriad of applications including ceramics/or catalysts. The relative composition of the metal oxides is crucial as it is used in the determination of the application for a metakaolin sample. In this study, four metakaolin samples were prepared and analyzed in comparative studies of the content of the oxide of the metals present in the samples. The samples were obtained from Okepella, Nigeria in West Africa. Calcination by thermal treatment was carried out at 750℃ followed by the dealumination process to reduce the Alumina content. The composition of four different metakaolin samples, namely C01, A6060, B6075 and C12090, were compared. The porosity and morphology of the metakaolin samples were also studied. Characterization carried out included X-Ray diffraction, Field Emission Scanning Electron Microscope, Energy Dispersive X-ray Spectroscopy, Fourier Transform Infrared Spectroscopy, and Digital Imaging. It was clear from the Energy Dispersive X-ray analysis that most of the oxides contained Silicon and Aluminium as the main components. Thus, the metakaolin samples were primarily composed of Silica and Alumina. Trace amounts of titanium, potassium and sodium were also observed in the samples studied. While three samples (C01, A6060, B6075) had an almost equal

amount of silica and alumina, metakaolin C12090 was composed of mainly Silica with only trace amounts of other elements and without the presence of Alumina. The sample C01 contained the highest amount of Aluminium (21.22%) with C12090 containing no Aluminium. On the other hand, C12090 contained the highest amount of silicon (36%).

Acknowledgements

References

[1] González, J. A., Carreras, A. C., & Ruiz, M. D. C. (2007). Phase transformations in clays and kaolins produced by thermal treatment in chlorine and air atmospheres. *Latin American Applied Research*, *37*(2), 133-139.

[2] Barrer, R. M., Baynham, J. W., Bultitude, F. W., & Meier, W. M. (1959). 36. Hydrothermal chemistry of the silicates. Part VIII. Low-temperature crystal growth of aluminosilicates, and of some gallium and germanium analogues. *Journal of the Chemical Society (Resumed)*, 195-208.

[3] Kirk, R. E.; Othmer, D. F. (1991) Encyclopedia of Chemical Technology, 4th ed.; John Wiley & Sons: New York.

[4] De Lucas, A., Uguina, M. A., Covian, I., & Rodriguez, L. (1992). Synthesis of 13X zeolite from calcined kaolins and sodium silicate for use in detergents. *Industrial & engineering chemistry research*, *31*(9), 2134-2140. https://doi.org/10.1021/ie00009a010

[5] Chandrasekhar, S., & Pramada, P. N. (2001). Sintering behaviour of calcium exchanged low silica zeolites synthesized from kaolin. *Ceramics International*, *27*(1), 105-114. https://doi.org/10.1016/S0272-8842(00)00049-3

[6] Colina, F. G., Esplugas, S., & Costa, J. (2002). A new extraction procedure for simultaneous quantitative determination of water-soluble metals in reaction products of clays and inorganic salts. *Clays and clay minerals*, *50*(3), 401-405. https://doi.org/10.1346/000986002760833774

[7] Murray, H. H. (2007). *Applied clay mineralogy: occurrences, processing and applications of kaolins, bentonites, palygorskitesepiolite, and common clays*. Elsevier. ISSN: 1572-4352

[8] White, C. E., Provis, J. L., Riley, D. P., Kearley, G. J., & Van Deventer, J. S. (2009). What is the structure of kaolinite? Reconciling theory and experiment. *The Journal of Physical Chemistry B*, *113*(19), 6756-6765. DOI: 10.1021/jp810448t

[9] Olaremu, A. G. (2015). Physico-chemical characterization of Akoko mined kaolin clay. *Journal of Minerals and Materials characterization and Engineering*, *3*(05), 353-361. http://dx.doi.org/10.4236/jmmce.2015.35038

[10] Murray, H. H. (1999). Applied clay mineralogy today and tomorrow. *Clay minerals*, *34*(1), 39-49. https://doi.org/10.1180/000985599546055

[11] Zhang, R., Alecrim, V., Hummelgård, M., Andres, B., Forsberg, S., Andersson, M., & Olin, H. (2015). Thermally reduced kaolin-graphene oxide nanocomposites for gas sensing. *Scientific reports*, *5*(1), 1-6. DOI: 10.1038/srep07676

[12] Zhang, K., Cui, Z., Xing, G., Feng, Y., & Meng, S. (2016). Improved performance of dye-sensitized solar cells based on modified kaolin/PVDF-HFP composite gel electrolytes. *RSC advances*, *6*(102), 100079-100089. DOI: 10.1039/C6RA19803A

[13] Murray, H. H., Harvey, C., & Smith, J. M. (1977). Mineralogy and geology of the Maungaparerua halloysite deposit in New Zealand. *Clays and clay minerals*, *25*(1), 1-5. https://doi.org/10.1346/CCMN.1977.0250101

[14] Badmus, B. S., & Olatinsu, O. B. (2009). Geophysical evaluation and chemical analysis of kaolin clay deposit of Lakiri village, southwestern Nigeria. *International Journal of Physical Sciences*, *4*(10), 592-606. https://doi.org/10.5897/IJPS.9000276

[15] Chandrasekhar, S., & Pramada, P. N. (1999). Investigation on the synthesis of zeolite NaX from Kerala kaolin. *Journal of Porous Materials*, *6*(4), 283-297. https://doi.org/10.1023/A:1009632606671

[16] Goodyear, J., & Duffin, W. J. (1961). An X-ray examination of an exceptionally well crystallized kaolinite. *Mineralogical magazine and journal of the Mineralogical Society*, *32*(254), 902-907. https://doi.org/10.1180/minmag.1961.032.254.05

[17] Gruner, J. W. (1932). The crystal structure of kaolinite. *Zeitschrift für Kristallographie-Crystalline Materials*, *83*(1-6), 75-88. https://doi.org/10.1524/zkri.1932.83.1.75

[18] Brindley, G. W., & Robinson, K. (1946). The structure of kaolinite. *Mineralogical magazine and journal of the Mineralogical Society*, *27*(194), 242-253. https://doi.org/10.1180/minmag.1946.027.194.04

[19] Sengupta, P., Saikia, P. C., & Borthakur, P. C. (2008). SEM-EDX characterization of an iron-rich kaolinite clay. IJEMS, 15, 812-818. ISSN: 0022-4456

[20] Hassan, U. J., & Abdu, S. G. (2014). Structural analysis and surface morphology of kaolin. *Sci. World J.*, *9*(3), 33-37.

[21] Środoń, J., Drits, V. A., McCarty, D. K., Hsieh, J. C., & Eberl, D. D. (2001). Quantitative X-ray diffraction analysis of clay-bearing rocks from random preparations. *Clays and Clay Minerals*, *49*(6), 514-528. https://doi.org/10.1346/CCMN.2001.0490604

[22] Goldstein, J. I., Newbury, D. E., Michael, J. R., Ritchie, N. W., Scott, J. H. J., & Joy, D. C. (2017). *Scanning electron microscopy and X-ray microanalysis*. Springer. https://doi.org/10.1007/978-1-4939-6676-9

[23] Lim, A. J. M. S., Syazwani, R. N., & Wijeyesekera, D. C. (2016, July). Impact of oriented clay particles on X-ray spectroscopy analysis. In *IOP Conference Series: Materials Science and Engineering*, 136 (1), 012012. IOP Publishing. doi:10.1088/issn.1757-899X

[24] Farmer, V.C. (1974) The Infrared Spectra of Minerals. Mineralogical Society Monograph, London. http://dx.doi.org/10.1180/mono-4

[25] Gardsden, J.A. (1975) Infrared Spectra of Minerals and Related Inorganic Compounds. Butterworth & Co Publishers, Ltd., London. ISBN 0-408-70665-1.

[26] Saikia, B. J., & Parthasarathy, G. (2010). Fourier transform infrared spectroscopic characterization of kaolinite from Assam and Meghalaya, Northeastern India. *J. Mod. Phys*, *1*(4), 206-210. doi: 10.4236/jmp.2010.14031.

[27] Caponi, N., Collazzo, G. C., Jahn, S. L., Dotto, G. L., Mazutti, M. A., & Foletto, E. L. (2017). Use of Brazilian kaolin as a potential low-cost adsorbent for the removal of malachite green from colored effluents. *Materials Research*, *20*, 14-22. https://doi.org/10.1590/1980-5373-MR-2016-0673

[28] Costa, E., De Lucas, A., Uguina, M. A., & Ruiz, J. C. (1988). Synthesis of 4A zeolite from calcined kaolins for use in detergents. *Industrial & engineering chemistry research*, *27*(7), 1291-1296. https://doi.org/10.1021/ie00079a033

[29] Benco, L., Tunega, D., Hafner, J., & Lischka, H. (2001). Ab initio density functional theory applied to the structure and proton dynamics of clays. *Chemical Physics Letters*, *333*(6), 479-484. https://doi.org/10.1016/S0009-2614(00)01412-3

[30] Nayak, P. S., & Singh, B. K. (2007). Instrumental characterization of clay by XRF, XRD and FTIR. *Bulletin of Materials Science*, *30*(3), 235-238.

[31] Parthasarathy, G., Kunwar, A. C., & Srinivasan, R. (2001). Occurrence of moganite-rich chalcedony in Deccan flood basalts, Killari, Maharashtra, India. *European Journal of Mineralogy*, *13*(1), 127-134. https://doi.org/10.1127/0935-1221/01/0013-0127

[32] Babel, S., & Kurniawan, T. A. (2003). Low-cost adsorbents for heavy metals uptake from contaminated water: a review. *Journal of hazardous materials*, *97*(1-3), 219-243. https://doi.org/10.1016/S0304-3894(02)00263-7

[33] Scorzelli, R. B., Bertolino, L. C., Luz, A. B., Duttine, M., Silva, F. A. N. G., & Munayco, P. (2008). Spectroscopic studies of kaolin from different Brazilian regions. *Clay Minerals*, *43*(1), 129-135. http://dx.doi.org/10.1180/claymin.2008.043.1.10

[34] Panda, A. K., Mishra, B. G., Mishra, D. K., & Singh, R. K. (2010). Effect of sulphuric acid treatment on the physico-chemical characteristics of kaolin clay. *Colloids and Surfaces A: Physicochemical and Engineering Aspects*, *363*(1-3), 98-104. http://dx.doi.org/10.1016/j.colsurfa.2010.04.022